

Porous media pressure distribution in centrifugal fields

W. L. Hogarth,¹ F. Stagnitti,² D. A. Barry,³ D. A. Lockington,⁴ L. Li,⁴ and J.-Y. Parlange⁵

Received 5 June 2013; revised 9 August 2013; accepted 14 August 2013; published 4 October 2013.

[1] The simplest use of centrifuges to measure soil properties relies on steady state conditions. Analytical solutions, especially if they are simple, make interpretation of data more direct and transparent. Previous approximations are simplified and have a greatly improved accuracy. Using previous examples as a test, the error on pressure is always less than 1%, compared to about 10% with previous approximations.

Citation: Hogarth, W. L., F. Stagnitti, D. A. Barry, D. A. Lockington, L. Li, and J.-Y. Parlange (2013), Porous media pressure distribution in centrifugal fields, *Water Resour. Res.*, 49, 7133–7138, doi:10.1002/wrcr.20487.

1. Introduction

[2] Starting with the pioneering work of *Alemi et al.* [1976], centrifuges have been a convenient tool to measure quickly soil properties. Effectively increasing the effect of gravity shortens the duration of experiments, although as a consequence, care must be taken so that measured capillary pressures have their static values [*Oung et al.*, 2005]. Most experiments have been carried out under steady state conditions for simplicity and reliability. Nimmo and coworkers [*Nimmo et al.*, 1987; *Nimmo*, 1990; *Simunek and Nimmo*, 2005; *Caputo and Nimmo*, 2005] adapted the steady state results to interpret transient experiments as well. Some applications are ideally suited for centrifuge, e.g., flow in fractures [*Levy et al.*, 2002]; colloids transport in porous media [*Sharma et al.*, 2008]; air sparging [*Marulanda et al.*, 2000]; geo-environmental problems [*Savvidou and Culligan*, 1998]. There have been many other important contributions to the field which are described in the careful review of *van den Berg et al.* [2009].

[3] To transfer results from the centrifuge to the prototype, scaling laws are required [*Culligan and Barry*, 1998; *Barry et al.*, 2001]. Interpretation of data is not easy and requires very careful numerical simulations [*Ataie-Ashtiani et al.*, 2003]. *Basha and Mina* [1999] pointed out the great advantage of analytical solutions, when attainable, because of their simplicity and transparency, and also if they can be

used as a check of the accuracy of the numerical solutions. *Basha and Mina* [1999] then offered an analytical approximation to be used for steady state measurements of unsaturated hydraulic conductivity with a centrifuge. This case is obviously the most fundamental and they knew full well that their solution was only a first step as it had only a 10% precision on the average and it required two different approximations to cover the whole range of properties. *Parlange et al.* [2001] suggested some minor improvement of the solution with further insight provided by *Basha* [2001]. However, the accuracy, though improved, was still not outstanding with a maximum error around 10%. In this paper, after several years, we are finally able to cover the whole range of conditions with a maximum error of less than 1%.

[4] Following *Basha and Mina* [1999], we write the steady state centrifuge equation as

$$\frac{d\phi}{dR} = -AR - D + C\phi^n \quad (1)$$

for a *Gardner* [1958] type of soil water conductivity, k ,

$$k/k_o = [a + b\phi^n]^{-1} \quad (2)$$

[5] We changed the signs of the constants A , C , and D so they are positive here. ϕ is the pressure relative to the pressure at the bottom of the column, $p_b < 0$, so $\phi_b = 1$ at $R = R_b$. R is the distance from the axis of the centrifuge measured in units of the length L of the column so that the top of the column is closer than the bottom to the axis of rotation, i.e., $R_t < R_b$, and k_o is a characteristic conductivity value. With w the angular velocity and q the flux density,

$$-A = L^2 w^2 / gp_b; -B = qL / k_o p_b; D = aB; C = bB \quad (3)$$

[6] Note that if $a = 0$, the D term in equation (1) is equal to zero, if $a \neq 0$, the D term can always be absorbed in the AR term by changing the position of $R = 0$. In the following, we drop the D term without any loss of generality.

[7] A in equation (3) represents the relative importance of centrifugal and capillary forces, whereas B or C shows the impact of the flux density, i.e., with $B = C = 0$, the

¹Faculty of Science and IT, University of Newcastle, Callaghan, New South Wales, Australia.

²DVC Research, University of Ballarat, Ballarat, Victoria, Australia.

³Ecole polytechnique fédérale de Lausanne, Faculté de l'environnement naturel, architectural et construit, Institut d'ingénierie de l'environnement, Lausanne, Switzerland.

⁴School of Civil Engineering and National Centre for Groundwater Research and Training, University of Queensland, St Lucia, Queensland, Australia.

⁵Department of Biological and Environmental Engineering, Cornell University, Ithaca, New York, USA.

Corresponding author: J.-Y. Parlange, Department of Biological and Environmental Engineering, Cornell University, Ithaca, NY 14853, USA. (jp58@cornell.edu)

Table 1. Parameters Necessary to Plot the Analytical Results for *Basha and Mina* [1999], Examples in Figure 3 for $n = 2$ and Figures 5 and 6 for $n = 5$, With Three Below the Asymptote, $f(r)$, and One Above in Each Case^a

$n = 2$		C	A	f_1	r_1	Ψ_1	r_2	g_1/g_{r_0}		
$\psi < f$	0.5	1	1.854	3.175	0.630	2.381	0.493			
$\psi < f$	0.5	3	2.192	4.579	0.437	3.434	0.667			
$\psi < f$	5	1	2.651	9.864	2.028	7.398	–			
$\psi > f$	5	3	3.165	6.840	2.924	5.130	0.219			
$n = 5$		C	A	β^{-1}	λ	f_1	r_1	Ψ_1	r_2	$10^{-3}g_1/g_{r_0}$
$\psi < f$	0.5	1	0.367	79.055	1.304	3.704	0.857	2.777	24.43	
$\psi < f$	0.5	3	0.393	58.917	1.435	6.035	0.759	4.526	56.55	
$\psi < f$	5	1			1.371	7.794	1.266	5.846	–	
$\psi > f$	5	3	0.339	114.267	1.509	4.783	1.430	3.588	5.718	

^aFor the two cases above, the asymptotes are for, $r_\infty = 7.403(n = 2)$; $r_\infty = 4.899(n = 5)$ and $f_\infty = 2.754(n = 2)$; $f_\infty = 1.377(n = 5)$.

equilibrium pressure is obtained when centrifugal and capillary forces balance each other with no flow.

[8] A first important step is to reduce the number of parameters from three (R_b , A , and C) to two by relinquishing the condition that the length of the column be taken as unit of length. To do so, we change variables taking:

$$R = \alpha_1 r; \phi = \alpha_2 \psi \tag{4}$$

with

$$\alpha_1 = [A^{n-1}C]^{-1/(2n-1)}; \alpha_2 = [A/C^2]^{1/(2n-1)} \tag{5}$$

$$d\psi/dr = \psi^n - r \tag{6}$$

with boundary condition,

$$\psi = \psi_1, \text{ at } r = r_1 \tag{7}$$

r_1 and ψ_1 are now the only two parameters entering the problem.

[9] We take the examples of *Basha and Mina* [1999], which cover a wide range of conditions, i.e., $A = 1$ and 3; $C = 5$ and 0.5; with $n = 2$ and 5, eight cases altogether. Their boundary condition, equation (3), was for $R_b = 4$. Table 1 gives the corresponding values of r_1 and ψ_1 , as well as r_2 , which is the top of the column at $R_t = 3$.

[10] To solve equation (6), we have to consider two regions separately, an upper and lower region. Those two regions are separated by a boundary $\psi = f(r)$ where f still obeys equation (6) but satisfies the condition

$$df/dr = 0 \text{ as } r \rightarrow \infty \tag{8}$$

[11] For r large, $f^n \simeq r$, and using this estimate to calculate df/dr , we obtain to the first order

$$r = f_1^n - \frac{1}{nf_1^{n-1}} \tag{9}$$

and to the second order, using the first order to calculate df/dr ,

$$r = f_2^n - \frac{1}{nf_2^{n-1} \left[1 + \frac{n-1}{n^2 f_2^{2n-1}} + \dots \right]} \tag{10}$$

[12] Higher-order terms could easily be calculated, but will not be found necessary. Clearly, equations (9) and (10) should be accurate when r is large; however, we would like to find an accurate $f(r)$ down to $r = 0$. Using this value of $r = 0$ as a check, we can find $f_{10} = f_1(r = 0)$ and $f_{20} = f_2(r = 0)$. Table 2 gives those values for $n = 2, 3, 4, 5$, as well as the value obtained numerically. We find that f_{20} is always too small and f_{10} too large, suggesting that some ‘‘average’’ would be more accurate. In equation (11), the geometric average of the second terms in equations (9) and (10) were used, giving the value f_0 at $r = 0$, shown in equation (12)

$$r = f^n - \left\{ nf^{n-1} \left[1 + (n-1)/(n^2 f^{2n-1}) \right]^{1/2} \right\}^{-1} \tag{11}$$

yielding,

$$2nf_0^{2n-1} = -\frac{n-1}{n} + \left[4 + \left(\frac{n-1}{n} \right)^2 \right]^{1/2} \tag{12}$$

[13] Note that f_0 , and f in general, are physically positive; hence the negative solution of equation (11) can only have a mathematical meaning when n is a positive integer. Table 2 shows the excellent accuracy of equation (12). Note that for the two limits, $n = 1$ and $n \gg 1$, equation (12) predicts the exact value of f_0 . With the example of $n = 2$, we shall discuss the negative branch later, again for mathematical interest. The value of n can only be known approximately so if it were to change from an even integer value to an infinitesimally close value, the negative branch would suddenly disappear, confirming that the negative branch is not relevant physically.

[14] To solve equation (6), either above or below the boundary, $f(r)$, we consider the case when part of $\psi(r)$ is

Table 2. Values of $f_{20} = f_2(r = 0)$; $f_{10} = f_1(r = 0)$ From Equations (10) and (9) for Various n^a

n	f_{20}	f_{10}	Numerics	Equation (12)
2	0.630	0.794	0.7290	0.7309
3	0.644	0.803	0.7521	0.7519
4	0.673	0.820	0.7793	0.7785
5	0.699	0.836	0.8018	0.8008

^aThe corresponding numerical results and the predictions of equation (12) are also given.

close to $f(r)$. For that case, we rewrite equation (6) as

$$d[\psi - f]/dr = \psi^n - f^n \quad (13)$$

and linearize that equation to obtain

$$d[(\psi^\beta - f^\beta)\psi_a^{1-\beta}]/dr = (\psi^\beta - f^\beta)n\psi_a^{1-\beta}\psi_c^{n-1} \quad (14)$$

where ψ_a and ψ_c are between ψ and f , to be chosen later. The solution of equation (14) can be written as

$$\psi^\beta - f^\beta = \beta\psi_a^{\beta-1}\lambda \exp \int^r n\psi_c^{n-1} dr \quad (15)$$

[15] No lower limit was put in the integral as any change could always be absorbed by a new constant λ . We now choose ψ_a by a simple interpolation between ψ and f , e.g.,

$$\psi_a^{\beta-1} \simeq \psi^\beta f^{-1} \lambda_1/\lambda + f^{\beta-1} \lambda_2/\lambda \quad (16)$$

where λ_1 and λ_2 are constants to be obtained later. Using ψ_a from equation (16) in equation (15) yields

$$\frac{\psi^\beta}{f^\beta} = \frac{1 + \beta\lambda_2 f^{-1} \exp n \int f^{n-1} dr}{1 - \beta\lambda_1 f^{-1} \exp n \int f^{n-1} dr} \quad (17)$$

where we used $\psi_c \simeq f$, i.e., the asymptotic approximation for large r when ψ and f can differ the most.

[16] To estimate λ_1 , λ_2 , and β , we first look at the zeros of the denominator in equation (17), where $\psi \rightarrow \infty$ at $r = r_\infty$. Equation (6) shows that when this happens, $d\psi/dr \simeq \psi^n$, around r_∞ , then $(r_\infty - r)^{-1}$ behaves like $\psi^{n-1}(n-1)$, which is only possible if $\beta = n-1$ and equation (17) gives for $r \sim r_\infty$,

$$\psi^{n-1} \simeq \frac{1 + \lambda_2/\lambda_1}{(r_\infty - r)n} \quad (18)$$

where we used $dr/df \simeq nf^{n-1}$. Hence, $1 + \lambda_2/\lambda_1 = n/(n-1)$ or

$$\lambda_1/\lambda_2 = (n-1) \quad (19)$$

[17] Using now equation (9) to calculate dr in the integral $\int f^{n-1} dr$ in equation (17) (higher-order terms could also be used) yields

$$\frac{\psi^{n-1}}{f^{n-1}} = \frac{1 + g/(n-1)}{(1-g)} \quad (20)$$

with

$$g = (f/f_\infty)^{n-2} \exp \left[\frac{n^2}{2n-1} (f^{2n-1} - f_\infty^{2n-1}) \right] \quad (21)$$

where f_∞ is the value of f at r_∞ .

[18] Since the solution is only physical for $\psi > 0$, equation (20) applies to the upper region, i.e., above the boundary given by $f(r)$.

[19] If the boundary condition is below that boundary, no asymptote is available to find β . As a result, determination of the solution is more difficult to obtain. We take the boundary condition as

$$\psi = \psi_1, \text{ at } r = r_1 \quad (22)$$

and define g , following equation (21) as

$$g/g_1 = (f/f_1)^{n-2} \exp \left[\frac{n^2}{2n-1} (f^{2n-1} - f_1^{2n-1}) \right] \quad (23)$$

where $f_1 = f(r_1)$ and g_1 is a constant, with $g(r_1) = g_1$. As in the case above the boundary, we could try

$$\psi/f = \left(\frac{1 - \lambda_2 g}{1 + \lambda_1 g} \right)^{1/\beta} \quad (24)$$

[20] Note we change the signs of the λ 's as ψ can be zero but not infinite in that region. However, $\psi = 0$, at $r = r_0$, and $d\psi/dr = -r_0$ is finite and nonzero so equation (24) can apply only if we keep β in the denominator only, then

$$\psi/f \simeq [1 - g/g_{r0}]/[1 + \lambda g/g_{r0}]^{1/\beta} \quad (25)$$

with $\lambda/g_{r0} = \lambda_1$ and $g_{r0} = 1/\lambda_2$ value of g at $r = r_0$. To satisfy the derivative condition at $r = r_0$, requires at once,

$$1 + \lambda = n^\beta \quad (26)$$

which gives λ quite easily once β is known. Imposing that, equation (25) satisfies the derivative of ψ at $r = r_1$, gives

$$f_1^n - \psi_1^n = n f_1^{n-1} \psi_1 \frac{g_1}{g_{r0}} \left[\frac{1}{1 - \frac{g_1}{g_{r0}}} + \frac{\lambda/\beta}{1 + \lambda \frac{g_1}{g_{r0}}} \right] \quad (27)$$

[21] Starting at (ψ_1, r_1) , equation (11) yields f_1 ; then equations (26), (27), and (25) at $r = r_1$, relate the three unknowns: λ , β , and g_1/g_{r0} (note that g_{r0} is irrelevant and could be taken equal to 1 without loss of generality). Note also that if by chance $\psi_1(r_1) = 0$, i.e., $r_1 = r_0$, then equation (27) reduces to equation (26) and we are short one equation. In that case, we would impose that the second derivative is satisfied at $r_1 = r_0$, or

$$1 - 1/n^\beta = \beta/2 \quad (28)$$

[22] Obviously, equation (28) would be far easier to use than equation (27) but being a second derivative condition, it is less accurate than a first derivative condition when $\psi_1 \neq 0$.

2. Application to the Examples of Basha and Mina

[23] Examples are for $n = 2$, about the minimum value for a clay, and $n = 5$, typical value for a sand [Basha and Mina, 1999]. As explained earlier, integer values, especially even ones, give negative branches, $\psi < 0$, which are

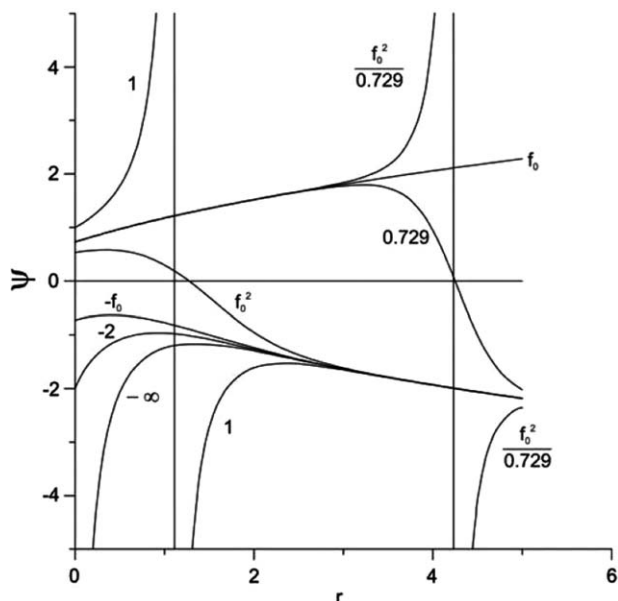


Figure 1. Exact solutions $\psi(r)$ for $n = 2$ at different starting points at $r = 0$, with $f_0 = -A'_{i0}/A_{i0}$. Only values for $\psi(r) \geq 0$ have physical meaning.

not physical, but will be touched upon here for mathematical completeness. Among even integers, $n = 2$ has an exact solution expressible in terms of Airy functions. Others values of n yielding exact analytical solutions are $n = 0; 1/2$ and 1 which are not considered here, as they are too small to have physical meaning.

[24] For $n = 2$, we can write exactly,

$$\psi = \left[-A'_i(r) - \mu B'_i(r) \right] / \left[A_i(r) + \mu B_i(r) \right] \quad (29)$$

[25] A_i and B_i being the two Airy functions, with

$$\mu = \left[-\psi_0 A_{i0} - A'_{i0} \right] / \left[+\psi_0 B_{i0} + B'_{i0} \right] \quad (30)$$

[26] Note that here the subscript “0” refers here to values at $r = 0$, and not to values at $r = r_0$.

[27] The case $n = 2$ is also unique as equations (26) and (27), together with equation (25) at $r = r_1$, yield $\lambda = \beta = 1$, which is also in agreement with equation (28).

[28] Figure 1 shows a variety of curves for $n = 2$, differing from their starting value at $r = 0$; from the top (as indicated on the figure) with $f_0 = -A'_{i0}/A_{i0} = B'_{i0}/B_{i0}$, $\psi_0(r = 0) = 1; f_0^2/0.729; f_0; 0.729; f_0^2; -f_0; -2; -\infty; 1; f_0^2/0.729$. Note that the curves $[1; f_0^2]$ and $[0.729; f_0^2/0.729]$ are such that the product of their $\psi_0(r = 0)$ is equal to f_0^2 . In that case, according to equations (20) and (25), f_0 and f_∞ and hence r_0 and r_∞ , should be the same as long as they are large enough for our asymptotic calculations to hold. Clearly, this is true when $r_0 \approx r_\infty \approx 4$ but not for $r_0 \sim r_\infty \sim 1$ as expected. Figure 2 compares numerical and analytical solutions for the Basha and Mina cases for $n = 2$ (each curve is identified by the value of ψ_1). When equation (6) is used, the comparison includes the nonphysical region of $\psi < 0$, with essentially no discrepancy. Figure 3 repeats the comparison with equation (1), and $D = 0$,

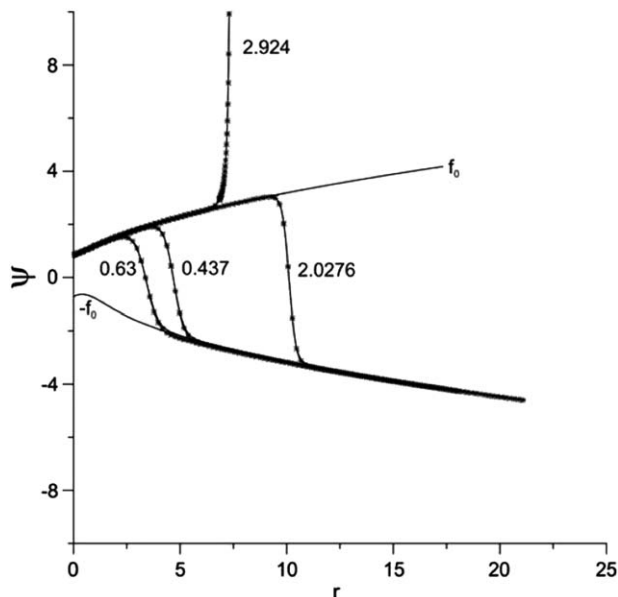


Figure 2. Four cases for $n = 2$, following the example of Basha and Mina [1999]. Numbers for each curve identify the starting values ψ_1 , see Table 1. Solid lines are the numerical results and the dots are the analytical results. The two asymptotes labeled $\pm f_0$ correspond to $\mu = 0$ and $\mu \rightarrow \infty$ in equation (29). Although the agreement of numerics and analysis is excellent, between the two asymptotes, only for $\psi \geq 0$ are the results physically meaningful.

showing more details; of course, the agreement is excellent.

[29] Figure 4 shows the general mathematical case for $n = 5$ including $\psi < 0$, which, again, would not be present

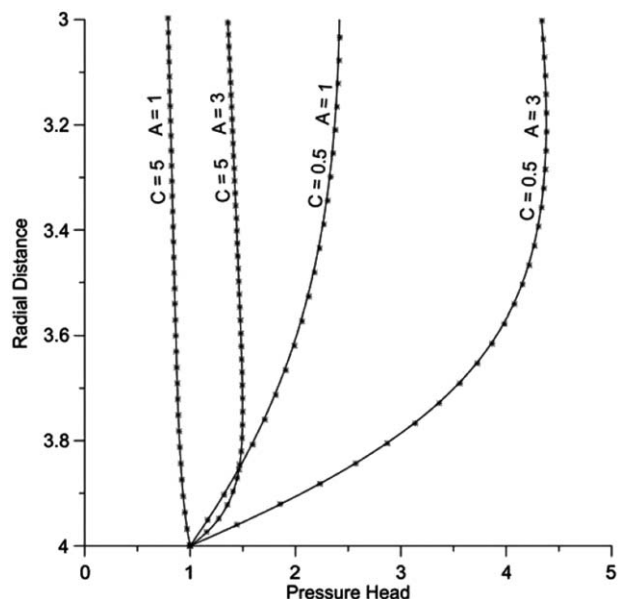


Figure 3. Details of the examples of Basha and Mina [1999] using the variables of equation (1), with $D = 0$, for $n = 2$. The solid lines are the numerical results and dots the analytical results.

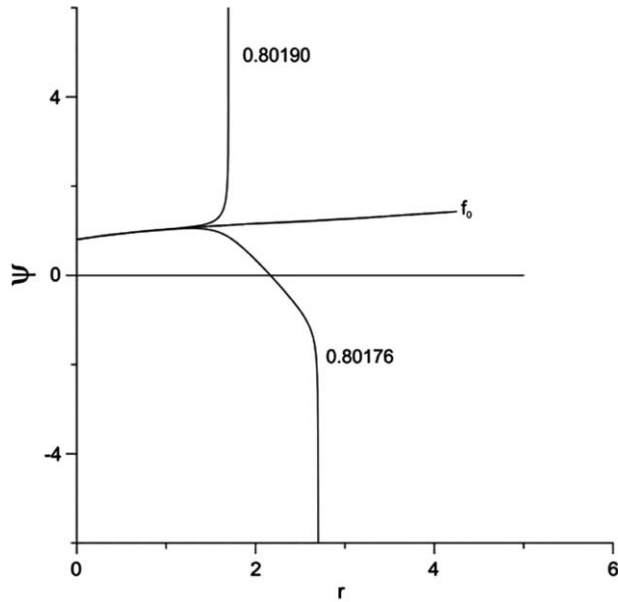


Figure 4. Sketch of two curves for $n = 5$, identified by the value of ψ_0 , one slightly above f_0 , one slightly below (for this last one, only the part with $\psi \geq 0$ is physically meaningful). In this case, n being an odd integer, there is only one asymptote $f(r)$ starting at f_0 .

if n was not an integer. The figure is much simpler than the corresponding one for $n = 2$ because only even integers have a solution $f < 0$. Figure 5 shows the comparison between the numerics and the analysis using equation (1) when equation (28) rather than equation (27) is applied which greatly simplifies the calculation. The figure shows that for C small, the maximum error is around 3%, more than the chosen threshold of 1%. The difficulty of taking

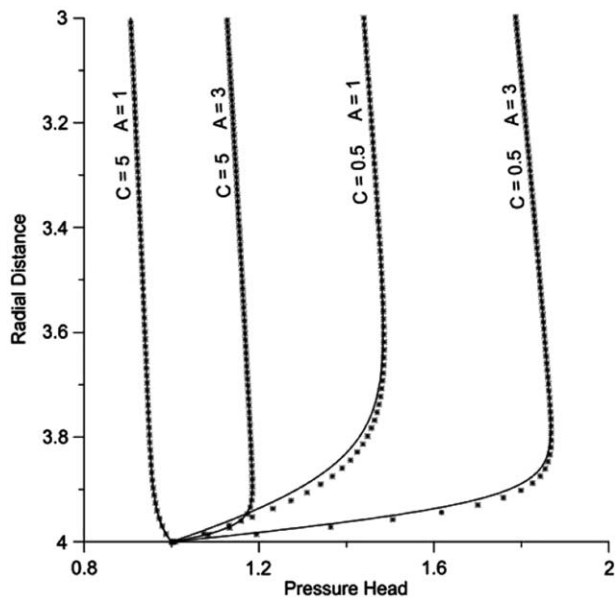


Figure 5. Details of *Basha and Mina's* [1999] cases for $n = 5$ when the simple equation (28) is used, showing the significant error when C is small. The analysis is shown by dots and the numerics by solid lines.

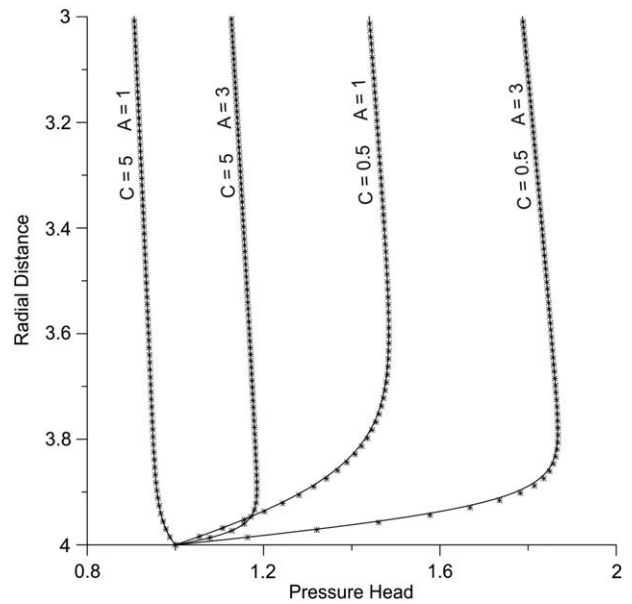


Figure 6. Same cases as in Figure 5 using equation (27), rather than equation (28). The errors for the cases with C small have disappeared. The analysis is shown by the dots and the numerics by the solid lines.

either equation (27) or (28) to estimate β did not appear for $n = 2$, as both gave at once $\beta = 1$. Figure 6 shows that when equation (27) is applied, the error disappears, which is natural since the derivative condition is applied where the boundary condition is used rather than a curvature condition at $\psi = 0$.

[30] In all cases, equation (11) is used to obtain r for a given f . However, for a given r to obtain f , we used an iterative procedure. We start with $f^n \approx r$ and use this value to obtain an estimate of the term in the $\{\}$ bracket in equation (11) and use the new estimate of f^n thus obtained to repeat the procedure. Numerically, equation (6), with $\psi = f$, is integrated using a Runge-Kutta procedure, starting with $f_1 = r_1^{1/n}$ where r_1 is very large, larger than any r of interest, e.g., $r_1 = 10$. Integrating backward, the asymptote is approached very quickly, yielding a stable solution. Forward integration, starting at a point very close to the asymptote, yields an unstable solution which eventually diverges from the asymptote. This is clearly seen in Figure 1, where the curves starting at $r = 0$ with ψ equal to 0.729 and $f_0^2/0.729$, which are close to the exact value of $f_0 = 0.7290111\dots$ still diverge at the short distance when $r > 3$.

[31] The values of f_∞ and r_∞ in Table 1, i.e., the asymptotes when $\psi \triangleright f$, are obtained starting from the boundary condition $\psi = \psi_1$ at $r = r$. As explained above, f_1 is then calculated and g_1 is obtained from equation (20). Using those values in equation (21) yields f_∞ and then r_∞ from equation (11).

3. Conclusion

[32] We have obtained an extremely accurate approximation to predict pressure in a centrifuge for steady state conditions when conductivity is a power law of pressure.

The accuracy makes the use of the solution quite reliable to predict soil water properties. The two difficulties in previously available approximations, i.e., using two different approximations depending on soil water properties, and limited accuracy, have been resolved. Here, the form of the approximation depends only on whether $\psi(r_1)$ is greater or less than $f(r_1)$.

References

- Alemi, M. H., D. R. Nielsen, and J. W. Biggar (1976), Determining hydraulic conductivity of soil cores by centrifugation, *Soil Sci. Soc. Am. J.*, 40(2), 212–218.
- Ataie-Ashtiani, B., S. M. Hassanizadeh, O. Oung, F. A. Weststrate, and A. Bezuijen (2003), Numerical modelling of two-phase flow in a geocentrifuge, *Environ. Modell. Software*, 18(3), 231–241.
- Barry, D. A., I. G. Lisle, L. Li, H. Prommer, J.-Y. Parlange, G. C. Sander, and J. W. Griffioen (2001), Similitude applied to centrifugal scaling of unsaturated flow, *Water Resour. Res.*, 37(10), 2471–2479.
- Basha, H. A. (2001), Reply to comment by H. A. Basha and N. I. Mina on “Estimation of the unsaturated hydraulic conductivity from the pressure distribution in a centrifugal field,” *Water Resour. Res.*, 37(1), 173–174.
- Basha, H. A., and N. I. Mina (1999), Estimation of the unsaturated hydraulic conductivity from the pressure distribution in a centrifugal field, *Water Resour. Res.*, 35(2), 469–477.
- Caputo, M. C., and J. R. Nimmo (2005), Quasi-steady centrifuge method for unsaturated hydraulic properties, *Water Resour. Res.*, 41, W11504, doi:10.1029/2005WR003957.
- Culligan, P. J., and D. A. Barry (1998), Similitude requirements for modelling NAPL movement with a geotechnical centrifuge, *Proc. Inst. Civ. Eng. Geotech. Eng.*, 131(3), 180–186.
- Gardner, W. R. (1958), Some steady-state solutions of the unsaturated moisture flow equation with application to evaporation from a water table, *Soil Sci.*, 85(4), 228–232.
- Levy, L. C., P. J. Culligan, and J. T. Germaine (2002), Use of the geotechnical centrifuge as a tool to model dense nonaqueous phase liquid migration in fractures, *Water Resour. Res.*, 38(8), doi:10.1029/2001WR000660.
- Marulanda, C., P. J. Culligan, and J. T. Germaine (2000), Centrifuge modeling of air sparging—A study of air flow through saturated porous media, *J. Hazard. Mater.*, 72(2-3), 179–215.
- Nimmo, J. R. (1990), Experimental testing of transient unsaturated flow theory at low water-content in a centrifugal field, *Water Resour. Res.*, 26(9), 1951–1960.
- Nimmo, J. R., J. Rubin, and D. P. Hammermeister (1987), Unsaturated flow in a centrifugal field: Measurement of hydraulic conductivity and testing of Darcy’s law, *Water Resour. Res.*, 23(1), 124–134.
- Oung, O., S. M. Hassanizadeh, and A. Bezuijen (2005), Two-phase flow experiments in a geocentrifuge and the significance of dynamic capillary pressure effect, *J. Porous Media*, 8(3), 247–257.
- Parlange, J.-Y., D. A. Barry, and L. Li (2001), Comment on “Estimation of the unsaturated hydraulic conductivity from the pressure distribution in a centrifugal field” by H. A. Basha and N. I. Mina, *Water Resour. Res.*, 37(1), 171–172.
- Savvidou, C., and P. J. Culligan (1998), The application of centrifuge modelling to geo-environmental problems, *Proc. Inst. Civ. Eng. Geotech. Eng.*, 131(3), 152–162.
- Sharma, P., M. Flury, and E. D. Mattson (2008), Studying colloid transport in porous media using a geocentrifuge, *Water Resour. Res.*, 44, W07407, doi:10.1029/2007.0163.
- Simunek, J., and J. R. Nimmo (2005), Estimating soil hydraulic parameters from transient flow experiments in a centrifuge using parameter optimization technique, *Water Resour. Res.*, 41, W04015, doi:10.1029/2004WR003379.
- van den Berg, E. H., E. Perfect, C. Tu, P. S. K. Knappett, T. P. Leao, and R. W. Donat (2009), Unsaturated hydraulic conductivity measurements with centrifuges: A review, *Vadose Zone J.*, 8(3), 531–547.